

**ENIGMATIC TUBULAR TEXTURES HOSTED IN IMPACT GLASSES FROM THE RIES IMPACT STRUCTURE, GERMANY.** H. M. Sapers<sup>1\*</sup>, G. R. Osinski<sup>1</sup>, and N. R. Banerjee<sup>1</sup>. <sup>1</sup>Centre for Planetary Science and Exploration & Dept. of Earth Sciences, University of Western Ontario, London, ON, N6A 5B7, Canada. \*E-mail: hsapers@uwo.ca.

**Introduction:** Impact cratering is a ubiquitous geological process on solid planetary bodies. Any hypervelocity impact into a H<sub>2</sub>O-rich target has the potential to generate hydrothermal systems [1]. Recent research has suggested that such impact-induced environments may be conducive to microbial colonization [e.g., 2]. In volcanic environments, bioalteration of basaltic glasses produces characteristic tubular and granular aggregate textures [e.g. 3]. Such bioalteration textures preserved in Archean greenstone belts constitute one of the oldest records of life on Earth [4]. Our examination of glasses from the Ries impact structure, Germany, has revealed tubular textures with remarkably similar morphologies to textures observed in volcanic glasses (Fig. 1).

Here we present preliminary data characterizing the putative bioalteration structures hosted within the Ries impact glasses. Establishing the biogenicity of the alteration structures observed in impact glasses has significant astrobiological implications, as impact cratering is a ubiquitous geological process throughout the solar system [e.g., 5,6].

**Impact glasses:** Impact glasses share many similarities with volcanic glasses; however, fundamental differences make impact glasses unique geochemical systems [7]. The bulk compositions of impact melts are diverse, reflecting heterogeneities in the target lithologies. Furthermore, impact melts often display heterogeneity on multiple scales. Given the probable ubiquity of impact glasses in hydrothermal settings throughout the Solar System, a better understanding of the habitability potential for hydrothermally altered impact glasses may provide insight into the possibility of similar microbial niches on other terrestrial planets, including Mars [6, 8].

**The Ries impact structure:** The  $14.3 \pm 0.2$  Ma [9] Ries impact structure, southern Germany, was formed in a two-layer target comprised of Mesozoic flat lying siliciclastic and carbonate sedimentary rocks that unconformably overlie crystalline Hercynian basement [10]. Ries is a complex crater with a total diameter of ~24 km [10]. Impactite and ejecta deposits are well preserved: surficial “suevite” comprises one of four main proximal ejecta deposits [11].

The surficial “suevites” (impact melt-bearing breccias) are divided into two distinct lithological units: 1) the dominant main suevite that represents a clast-rich particulate impact melt rock or impact melt-bearing breccia [11, 12]; 2) subordinate basal suevite [13]. Four main glass types occur within the main suevite both as groundmass phases and as discrete

glass clasts [7]. Glass clasts are typically vesiculated, schlieren-rich mixtures containing abundant mineral and lithic fragments [11]. The glass clasts hosted within the suevite have been classified based on composition and microtextures [7]. Type I glasses are the most abundant in the Ries suevites, contain Al-rich pyroxene quench crystallites and have SiO<sub>2</sub> contents ~63%. Type II glasses have a similar SiO<sub>2</sub> content as type I; however, they contain only plagioclase crystallites as well as a generation of dense, micron-scale vesicles. Type III glasses have low SiO<sub>2</sub> contents, are hydrated relative to the other glasses, and contain relatively little FeO, MgO, and K<sub>2</sub>O, while having high Al<sub>2</sub>O<sub>3</sub>, CaO, and Na<sub>2</sub>O contents. Type IV glasses have very high SiO<sub>2</sub> contents commonly >90%. Type I glasses have the highest concentrations of FeO and MgO of all 4 glass types [7].

**Glass alteration:** Evidence of a post-impact hydrothermal system at Ries has been documented [e.g., 14], but it has been suggested that this system was restricted to the crater-fill units [15]. Our recent examination of alteration of suevitic glasses suggests that alteration of glass clasts within the surficial suevite preserve evidence for alteration at variable temperatures as evidenced by varying mineral assemblages (see below) [16]. Alteration textures are spatially restricted and include colliform/rhythmic banding, amygdaloidal infilling, pervasive alteration/complete replacement of glass clasts by clay and the occurrence of coarse-grained, platy clays. Higher temperature autometamorphism and lower temperature weathering are more common, which is consistent with a limited hydrothermal system within the surficial suevites.

Focus is given to type I glasses as they comprise >90% of the glass clasts hosted within the Ries surficial suevite [7]. Suevites in general are defined based on the presence of type I glass clasts hosted within a cataclastic matrix. The fresh type I glass from Ries hosting the enigmatic tubular textures varies in colour from colourless to brown, yellow, pink or green; yellow-brown being dominant. The glass typically has a cloudy appearance, which increases with tubule density. High tubule density also optically darkens the glass. Increasing alteration and hydration also darkens the glass; highly altered glass clasts may appear dark brown to black through plane polarized light. The glass clasts are heterogeneous within samples and between samples. There is also variation within individual glass clasts. Mineral assemblages were interpreted by  $\mu$ XRD analysis and include: quartz, potassium feldspar, plagioclase, zeolites, calcic amphibole, phyllosilicates (bi-

otite, chlorite, illite and montmorillonite), carbonates (dolomitic), and sulphides (chalcopyrite).

The stability and corresponding cation release rates (metal availability) of natural glasses has implications for potential microbial colonization [e.g., 17]. It has been noted that bioalteration textures are more abundant in basaltic (Si-poor) glasses relative to rhyolitic (Si-rich) glass [e.g., 18]. The preferential microbial colonization of basaltic glass has been hypothesized to result from greater availability of bio-essential cations as well as easier dissolution of the glass.

**Enigmatic tubular textures:** Tubular textures have only been observed in type I and II Ries glasses and can be organized into 3 classes based on morphology and distribution. Class A tubules are commonly observed in both type I and II glasses, are either randomly distributed or concentrated around glass rims or vesicles, and have a relatively simple morphology with few complex curves. Class B tubules are observed only in type I glass, are concentrated along fractures or clast margins, form radiating aggregates, and have complex morphologies including spirals, and other complex curvatures. Class C tubules are observed only in one sample of type I glass. Class C tubules have significantly larger length to width ratios than other tubule classes and form straight, linear features in the glass.

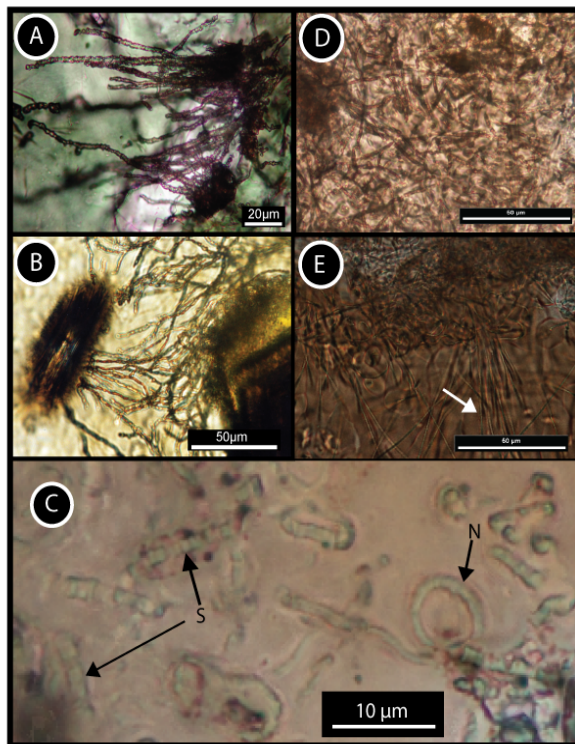


**Figure 1:** Tubular textures hosted in glass. A; Titanite mineralized segmented tubules in hyaloclastite from ~3.35Ga pillow basalt, Pilbara Craton, Western Australia [4]; B: Segmented tubular bioalteration in modern

basaltic glass, Ontong Java Plateau [3]; C, D E: Enigmatic tubular textures hosted in type I glass from surficial suevites of the Ries impact structure, Germany. C: Variation in morphology of class B tubules. Both segmented (S) and non-segmented (N) tubules are visible; D: Class B tubules; E: Class C tubules indicated by white arrow.

Class B tubules display various complex morphologies (Fig. 1). Approximately two-thirds do not display distinct segmentation. These smooth-walled tubules typically display complex curvatures forming a morphological continuum between loose undulating curves and spirochete morphology. Curvature appears random, non-oriented and specific to individual tubules. Non-segmented tubules have diameters ~1µm and commonly have length to width ratios >5. Approximately a third of class B tubules are clearly segmented. Segmented tubules typically display less curvature than non-segmented tubules. Individual segments have length to width ratios approximately 1:2. Segmented tubules vary in diameter from ~1µm to approaching 3µm. Rare segmented tubules with large (~3µm) diameters have segments with length to width ratios approaching 1:6. Additional metrics describing tubule morphology may allow for specific subclassification of class B tubules.

Class A tubules are likely the optical expression of vesicle generation within the type I and II glass clasts comprising the ‘hair-like’ structures described by [5]. Type C tubules may represent quench crystallites. The complex morphologies of type B tubules, however, lack a parsimonious abiotic or mineralogical explanation and are reminiscent of microbial alteration textures observed in submarine basaltic glasses [3].

**References:** [1] Naumov, M V. (2005) *Geofluids*, 5, 165-184. [2] Cockell, C. S., Lee, P. (2002) *Biological Reviews*, 77, 279-310. [3] Furnes, H. et al. (2007) *Precambrian Res.* 158, 156-176. [4] Banerjee, N. R. et al. (2007) *Geochim. Cosmochim. Acta.* 71, A58. [5] Izawa, M. R. M. et al. (2009) *Planet. Space Sci.* In press. [6] Banerjee N. R. et al. (2004) *LPSC XXXV* abstract # 1248. [7] Osinski G. R. (2003) *MAPS* 38(11), 1641-1667. [8] Cockell C. S., et al. (2005) *MAPS* 40(12), 1901-1914 [9] Buchner E. et al. (2003) *Int. J. Earth Sci.* 92, 1-6. [10] Pohl J. et al. (1977) In *Impact and explosion cratering*. Ed. Roddy D. J., et al. NY: Pergamon Press. pp. 343-404. [11] Engelhardt W. v. (1990) *Tectonophysics* 171, 259-273. [12] Osinski G. R. et al. (2004) *MAPS* 39, 1655-1683. [13] Bringemeier D. (1994) *Meteoritics* 29, 417-422. [14] Osinski G. R. (2005) *Geofluids* 5, 202-220. [15] Muttik N. (2008) *MAPS* 43, 1827-1840. [16] Sapers, H. M. et al., (2009) *MAPS* 44, 5175. [17] Banerjee, N. R., Muehlenbachs, K. (2003) *G<sup>3</sup>* 4(4) 1037-1059. [18] Cockell, C. et al. (2009) *Geobiology*. 7, 50-65.